Received September 9, 2021, accepted September 25, 2021, date of publication September 29, 2021,
date of current version October 7, 2021.

Digital Object Identifier 10.1109/ACCESS.2021.3116107

Effect of Segmented Thermal Aging on Defect Location Accuracy in XLPE Distribution Cables

BINGLIANG SHAN[1], SHUNING LI[1], LIYING YU[1], (Student Member, IEEE), WEI WANG[1], CHENGRONG LI[1], AND XIAOKAI MENG[2]

[1]State Key Laboratory of Alternate Electrical Power System With Renewable Energy Sources, North China Electric Power University, Beijing 102206, China
[2]Electric Power Research Institute, State Grid Shanxi Electric Power Company, Taiyuan 030000, China

Corresponding author: Wei Wang (kingway@ncepu.edu.cn)

This work was supported in part by State Grid Corporation of China under Grant 5102-201956301A-0-0-00.

ABSTRACT Frequency domain reflectometry (FDR) technologies could be applied to locate defects in cables effectively. Owing to the large space span and complex operating environment of the actual XLPE distribution cables, segmented thermal aging phenomenon occurs easily, causing the nonuniform distribution of electrical parameters along cables, which might affect the defect location accuracy ultimately. In this paper, the segmented thermal aging cable models were established and the effect of segmented-aging in XLPE distribution cables on defect location accuracy was explored based on simulation. It was found the floating range of defect location deviation in segmented thermal aging cable models could reach 10% of the whole cable length, which could not be ignored. Further research and analysis revealed that the defect location deviation in the segmented-aging cable mainly attributes to the differences of distributed wave velocities in the cable. On this basis, a correction coefficient of defect location M was put forward for the segmented-aging cable models established, which has achieved remarkable results. Finally, a segmented-aging cable model with a length of 119 m was built in the laboratory, and the validity for improving defect location accuracy by considering the differences of wave velocities was verified through experiments. Results show the defect location deviation can be reduced from 2.19% to 0.39% by introducing M.

INDEX TERMS Segmented-aging cable, frequency domain reflection, broadband impedance spectrum, defect location, electromagnetic wave velocity.

I. INTRODUCTION

XLPE distribution cables are the important parts of urban power distribution network, and they are prone to defects during long-term operation, threatening the safety of grid operation [1]–[3]. Since many distribution cables are laid underground, it is difficult to find and locate the defects in time and then eliminate these potential faults [4].

To solve the above problems, a series of defect location methods have been proposed and developed in recent years. Among them, frequency domain reflectometry (FDR) technologies represented by broadband impedance spectrum (BIS) [5]–[8] and reflection coefficient spectrum (RCS) [9], [10] have attracted more attention. Fantoni *et al.* first developed a method called the Line Resonance Analysis (LIRA) for defect location and cable condition monitoring based on BIS [11], [12]. Then the comparison of BIS and time domain reflectometry (TDR) for locating cable degradation was conducted by researchers, results shown that BIS possesses a higher sensitivity to the diagnosis of aging defects with smaller changes in electrical parameters, because the measurement signal based on FDR contains more high-frequency components [13], [14]. At the same time, the sensitivity or spatial resolution of defect location was found to be affected by the highest measurement frequency, which could not be increased without limit since higher measurement frequency would lead to more severe signal attenuation [6], [15], [16]. In order to solve the problem, the RCS method was further proposed, and it has been proved that on the premise of ensuring the sensitivity and accuracy of defect location, the requirement of measurement frequency band and sampling frequency could be reduced to a certain extent [9], [10]. To date, the location of impedance discontinuities formed by concentrated defects such as local damaged insulation

The associate editor coordinating the review of this manuscript and approving it for publication was Fabio Mottola.

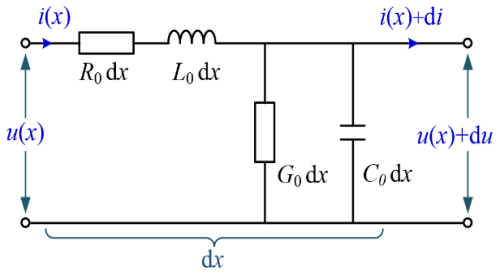

FIGURE 1. Distributed parameter model of power cables.

or joints affected with damp has been realized based on FDR [9], [17].

Though some progress has been made in defect location of XLPE distribution cables, the effect of segmented aging on defect location accuracy is rarely considered in existing studies, which may have some limitations in practical applications. In fact, segmented thermal aging phenomenon appears easily in actual XLPE distribution cables, owing to their large space span and complicated laying environment, it may affect the propagation process of measurement signal and defect location accuracy ultimately. No work focused on the effect of segmented-aging in XLPE distribution cables on defect location accuracy has been reported until now, which remains largely unclear. It would hinder the defect location accuracy as well as the elimination of potential insulation faults.

In this paper, the effect of segmented thermal aging on defect location accuracy in XLPE distribution cables was explored and demonstrated for the first time, through simulation and experimental research based on BIS. The cause of defect location accuracy was discussed, then a correction coefficient of wave velocity M was proposed to improve the defect location accuracy for the segmented-aging cable models established, and the validity of which has been verified. Study results in this paper can provide guidance and reference for more accurate location of defects in segmented-aging cables.

II. INPUT IMPEDANCE AND DEFECT LOCATION PRINCIPLE BASED ON BIS

A. INPUT IMPEDANCE OF CABLES

According to the transmission line theory [18], the distribution parameter model can be applied to describe the electrical network structure of power cable under high frequency power source, as illustrated in Figure 1. R_0, L_0, G_0 and C_0 represent the equivalent resistance, inductance, conductance and capacitance of power cable in per unit length, respectively, which can be calculated according to the material, size, structure and other parameters of cables [19].

For one power cable with a length of l and an open end, the input impedance Z_x at the distance x from the cable head end can be calculated as follows:

$$Z_x = Z_0 \left(\frac{1 + e^{-2\gamma x}}{1 - e^{-2\gamma x}} \right) \tag{1}$$

where f is the signal frequency, Z_0 and γ are respectively the characteristic impedance and propagation constant, which are given by:

$$Z_0 = \sqrt{(R_0 + j\omega L_0)/(G_0 + j\omega C_0)} \tag{2}$$

$$\gamma = \alpha + j\beta = \sqrt{(R_0 + j\omega L_0)\,(G_0 + j\omega C_0)} \tag{3}$$

where α and β are respectively the attenuation coefficient and propagation coefficient, then β can be obtained further by:

$$\beta = \frac{\omega}{v} = \frac{2\pi f}{v} \tag{4}$$

where v is the wave velocity propagating in the cable, ω is the angular frequency. Thus, the input impedance at the head end ($x = 0$) Z_{in} can be presented as follows:

$$Z_{\text{in}} = Z_0 \left(\frac{1 + e^{-2\gamma l}}{1 - e^{-2\gamma l}} \right) \tag{5}$$

B. CABLE DEFECT LOCATION PRINCIPLE BASED ON BIS

Previous studies have shown that the input impedance spectrum of coaxial cable varies approximately periodically with the signal frequency f [20], [21]. At high frequencies ($\omega L_0 \gg R_0$, $\omega C_0 \gg G_0$), Z_0 is almost independent of frequency and a constant, then it could be deduced reasonably that the periodicity of the input impedance spectrum is determined by $e^{-2\gamma l}$, according to the equation (5). Meanwhile, if another defect occurs at position $x = l_1$, the corresponding distribution parameter would be changed, and the periodicity of the input impedance spectrum would be also affected by $e^{-2\gamma l1}$ [20]. Adopting Euler equation, parameter $e^{-2\gamma l}$ could be expanded as follow:

$$e^{-2\gamma l} = e^{-2\alpha l} \times \left[\cos\left(\frac{4\pi f}{v} l \right) - j \sin\left(\frac{4\pi f}{v} l \right) \right] \tag{6}$$

Since α is the increasing function of f, $e^{-2\gamma l}$ can be regarded as an approximate periodic signal with $f'_{x=l} = 2l/v$ as the equivalent frequency though the amplitude is a decreasing function of the signal frequency f. Similarly, $e^{-2\gamma l1}$ can be regarded as an approximate periodic signal with $f'_{x=l1} = 2l_1/v$ as the equivalent frequency. Then the ratio of $f'_{x=l1}$ to $f'_{x=l}$ can be given as follows:

$$f'_{x=l_1}/f'_{x=l} = (2l_1/v)/(2l/v) = l_1/l \tag{7}$$

and l_1 can be calculated by equation (8).

$$l_1 = l \times \frac{f'_{x=l_1}}{f'_{x=l}} \tag{8}$$

Thus, extracting the characteristic parameters such as the amplitude spectrum or phase spectrum of the input impedance firstly, and then the equivalent frequency f' corresponding to the positions of cable defects and the end of the cable could be obtained by use of Fourier transform or integral transformation [8], [22]. On this basis, according to equation (8), the location of cable defects would be realized.

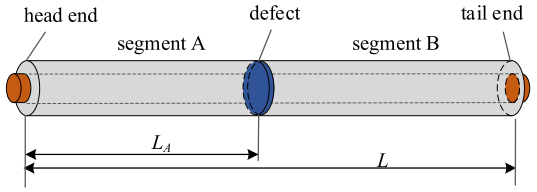

FIGURE 2. Schematic diagram of a segmented-aging cable model.

TABLE 1. Fitting parameters of the complex permittivity of cables with different thermal aging states [22].

Cable aging states	Fitting parameters		
	C	D/×10^{-9}	P
unaged	2.783	2.640	0.716
significantly aged	3.213	3.463	0.752
severely aged	4.232	8.560	0.832

III. STUDY ON THE EFFECT OF CABLE SEGMENT AGING ON DEFECT LOCATION ACCURACY BASED ON SIMULATION

A. MODEL AND SIMULATION PARAMETERS

In this paper, the 8.7/10 kV XLPE distribution cable was taken as an example to establish a segmented-aging cable model, as shown in Fig. 2. It consisted of segment A and segment B, and the total length and the length of segment A were L and L_A, respectively. The radius of the conductor was set to 10 mm, the thickness of the composite insulation (a synthesis of the XLPE layer and two semiconductor layers) and the metal shielding layer were respectively set to 4.5 mm and 0.2 mm. In addition, the impedance discontinuity at the junction of A and B was regarded as a cable defect, which was used to analyze and study the effect of cable segment aging on defect location accuracy.

The complex permittivity $\varepsilon(\omega)$ of the composite insulation layer (including the inner and outer semiconductor layers and the XLPE layer) of XLPE distribution cables with different thermal aging states was measured by literatures [20], [22]. Then $\varepsilon(\omega)$ was fitted according to Cole-Cole model as shown in Equation (9), since dipole polarization was the main polarization type for the composite insulation in the frequency range between 10 kHz and 100 MHz [23].

$$\varepsilon(\omega) = \frac{C\varepsilon_0}{1 + D(i\omega)^P} \tag{9}$$

Here, C, D and P are the fitting coefficients, and P $\in(0, 1)$, ε_0 is the vacuum dielectric constant. The corresponding fitting parameters obtained were shown in Table 1.

Therefore, the segmented-aging cable with different aging states could be simulated by changing the complex permittivity $\varepsilon(\omega)$ of segment A and segment B, according to Table 1. In this paper, A1, A2 and A3 represented that cable segment A was unaged, significantly aged and severely aged, respectively; similarly, B1, B2 and B3 represented that cable segment B was unaged, significantly aged and severely aged, respectively.

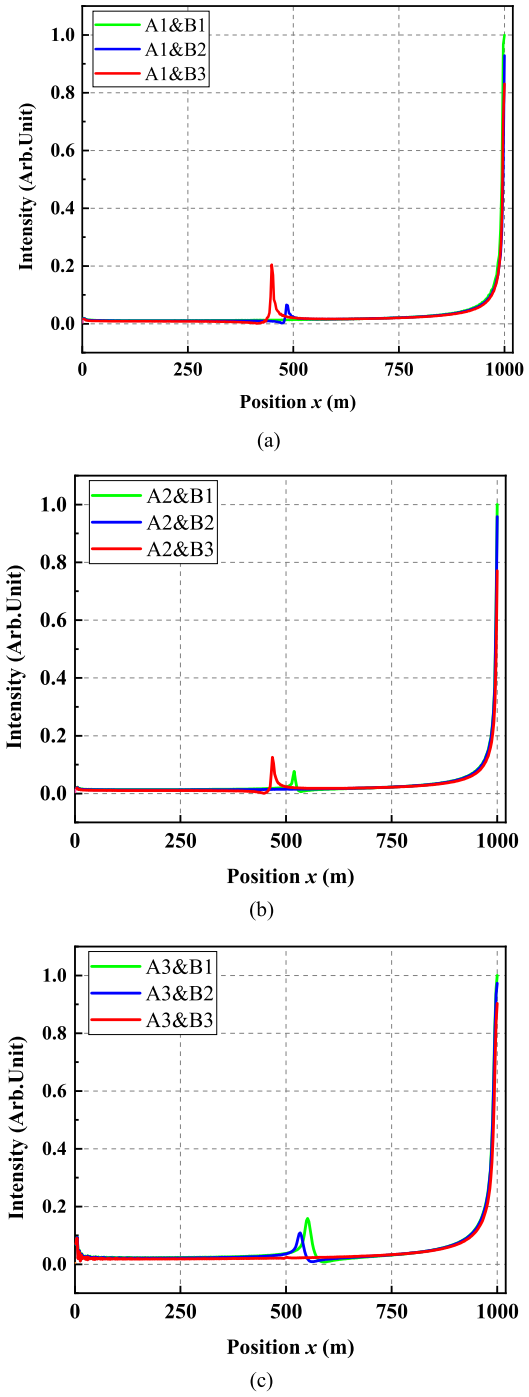

FIGURE 3. Diagnosis functions for the segmented-aging cable with different aging states.

B. SIMULATION RESULTS AND ANALYSIS

1) EFFECT OF THE AGING STATES OF CABLE SEGMENTS ON DEFECT LOCATION ACCURACY

L and L_A were set to 1000 m and 500 m, respectively, so the cable defect located at $x = 500$ m. Then the input impedance phase spectrum of the cable model was simulated when

TABLE 2. Deviation factor Q of cables with different aging states.

Deviation factor Q (%)	B1	B2	B3
A1	-	-1.64	-5.13
A2	1.94	-	-3.35
A3	5.13	3.37	-

segment A and segment B with different aging states referring to Table 1. Simulation frequency was in the range of 10 kHz to 100 MHz. Then the fast Fourier Transform (FFT) analysis was carried out to convert data obtained as a function of frequency f to those represented a function of the equivalent frequency f' to establish diagnostic functions. In addition, the x-coordinate of the peak formed by reflection at the tail end of the cable ($f'_{x=l}$) was set to 1000 m, and the final results was shown in Fig. 3.

A clear peak appears around the position $x = 500$ m when the aging state of segment A is different from that of segment B in Fig. 3, which indicates the cable defect at the junction of A and B could be recognized effectively. At the same time, it could be seen easily from the figure that the position of the peak formed by the cable defect deviates from its actual location. To quantitatively analyze the effect of the aging states of cable segments on defect location accuracy, a deviation factor Q was introduced, and it could be calculated according to equation (10).

$$Q = \left(\frac{f''}{f'} - \frac{l_1}{l}\right) \times 100\% \tag{10}$$

Based on it, the deviation factor Q of cables with different aging states was calculated and then shown in Table 2.

It is apparent in Table 2 that the deviation factor Q is in the range -5.13% to 5.13% accompanied with changes of aging states of segment A and segment B. Meanwhile, the greater the difference between the aging states of segment A and segment B, the larger the location deviation factor.

2) EFFECT OF THE CABLE LENGTHS ON DEFECT LOCATION ACCURACY

Since lengths of actual XLPE distribution cables are different from each other, the effect of the cable lengths on defect location accuracy was further studied. L was respectively set to 100 m, 1000 m, and 5000 m, while the ratio of L_A to L was controlled to 0.5. Considering the attenuation characteristics of the high-frequency signal transmitting along cables, the simulation frequencies of input impedance phase spectrum ranges were respectively taken as 10 kHz - 100 MHz, 10 kHz - 15 MHz, and 10 kHz - 2.5 MHz. During simulation, the aging states of the cable model were set to 4 cases: A1&B2, A1&B3, A2&B1, and A3&B1. Referring to the previous calculation process, the deviation factor Q could also be calculated, and Fig. 4. shows the final results.

As can be seen, the difference of cable length has little effect on the deviation factor Q, though Q varies with the aging states of cable segments.

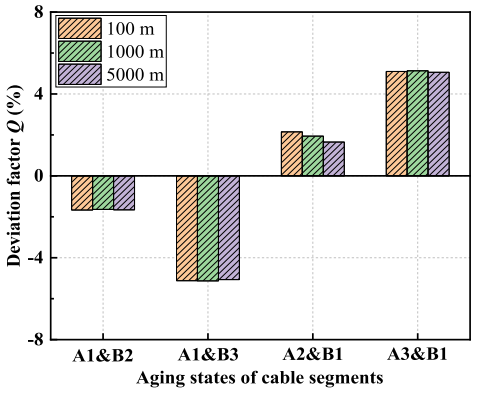

FIGURE 4. Defect location deviation of cables with different lengths.

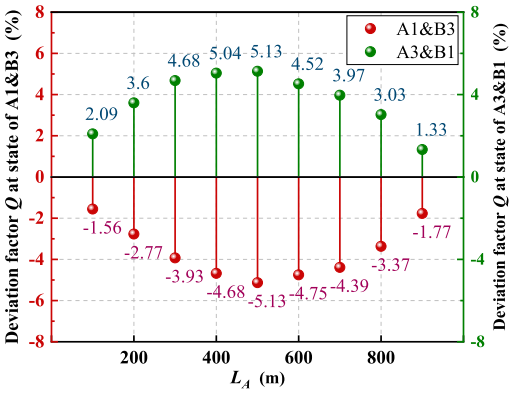

FIGURE 5. Defect location deviation of cables with different length percentages of aging segment.

3) EFFECT OF THE LENGTH PERCENTAGES OF AGING SEGMENT ON DEFECT LOCATION ACCURACY

The length percentage of aging segment in the actual cable was uncertain, which may affect the defect location accuracy. The input impedance phase spectrum of the segmented-aging cable with length $L = 1000$ m was simulated, while L_A varied from 100 m to 900 m at an interval of 100 m. The simulation frequency was in the range of 10 kHz to 15 MHz. Considering the typicality and simplicity of simulation objects, A1-B3 and A3-B1 were selected as the cable aging states. Finally, a summary of the defect deviation factors obtained were illustrated in Fig. 5.

Fig. 5 presents a reasonable relationship between the length L_A and the deviation factor Q. As L_A increases, the absolute value of Q presents a trend of increasing first and then decreasing, and the maximum absolute value of Q was 5.13% and it appears when $L_A = 500$ m. In addition, when the aging state of segment A is more serious than that of segment B, Q is a positive value; otherwise, it would be a negative value.

In summary, one conclusion could be drawn reasonably that the aging state and the length percentage of aging cable segments have a significant impact on defect location accuracy, while the cable length has almost no effect. Meanwhile, Q is normally in the range of -5.13% to 5.13%, which means that the floating range of defect location deviation could reach

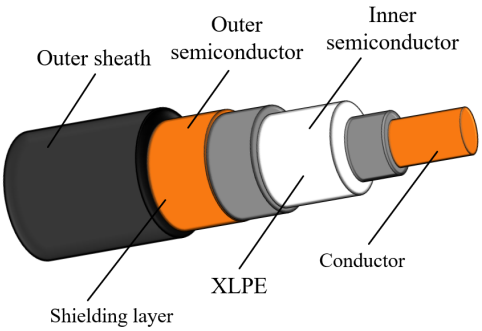

FIGURE 6. Structure diagram of XLPE cables.

about 10% of the whole cable length at most. The above results indicate that the effect of segmented-aging in cables on defect location accuracy could not be ignored, especially for the actual XLPE distribution cables whose length are usually several kilometers.

C. CAUSES OF DEFECT LOCATION DEVIATION

Fig. 6 illustrates the structure of an 8.7/10 kV XLPE distribution cable, which is mainly composed of the conductor, the inner and outer semiconductor layers, the XLPE layer, the shielding layer and the outer sheath. Thus, the capacitance of composite insulation layer mentioned previously C_{equal} consists of three components: capacitances of the inner and out semiconductor layers (C_{in}, C_{out}), and the capacitance of XLPE insulation layer C_{XLPE}. Their relationship could be expressed as follows:

$$\frac{1}{C_{equal}} = \frac{1}{C_{in}} + \frac{1}{C_{out}} + \frac{1}{C_{XLPE}} \tag{11}$$

Literature [24] has found that degradation of the cable insulation does have an impact on C_0 and at a lesser degree on the cable inductance L_0. In brief, the occurrence of water tree in XLPE insulation would promote significantly the number increase of polar groups and space charges, enhancing the relaxation polarization process; likewise, thermal aging of XLPE insulation would contribute to the break of XLPE molecular chains and formation of low molecular weight products, aggravating the interface relaxation polarization [22] and [25]. As a result, C_{XLPE} would increase. Ignoring the changes of C_{in} and C_{out} during cable aging, the above degradation phenomenon would result in the increase of C_{equal}.

Meanwhile, at high frequencies, the electromagnetic wave velocity v in XLPE cables is almost independent of the frequency f, which can be calculated as follows [26]:

$$v = \frac{1}{L_0 C_0} \tag{12}$$

Therefore, it could be deduced that the cable insulation aging would lead to the decrease of v ultimately. Equation (13) presents the corresponding frequency of the k'th maximum value of the input impedance amplitude spectrum

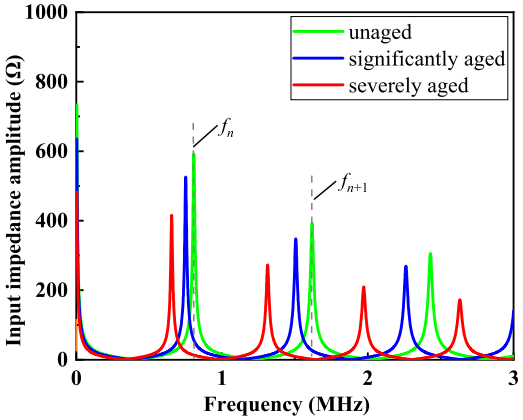

FIGURE 7. Input impedance amplitude spectrum of the uniform-aging cable with different aging states.

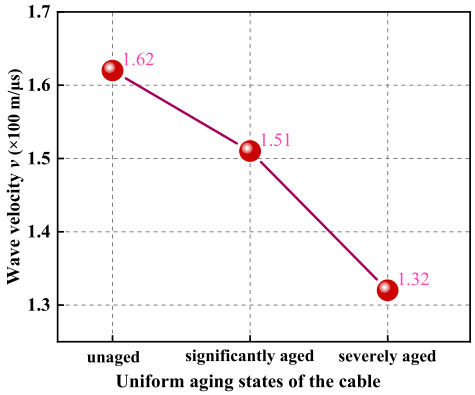

FIGURE 8. Wave velocity of the cable with different aging states.

with the tail end of the cable open [22]. Then the wave velocity v in the cable could be calculated according to equation (14).

$$f_{|Z_{in}|_{\max}} = k\frac{v}{2l}, \quad (k = 1, 2, 3\ldots) \tag{13}$$

$$v = (f_{n+1} - f_n) \times 2l, \quad (n = 2, 3, 4\ldots) \tag{14}$$

where, f_{n+1} and f_n are the adjacent frequency values corresponding to the maximum values of the input impedance amplitude spectrum. To further verify the effect of cable thermal aging on the wave velocity v, the input impedance amplitude spectrum of a uniform-aging cable with three kinds of aging states and a length of 100 m according to Table 1 was simulated, respectively. Fig. 7 presented the simulation results.

Combined with equation (14), wave velocities of the cable with different aging states were calculated, as shown in Fig. 8. As can be seen intuitively, the more serious aging state of the cable, the lower the wave velocity in the cable. For example, wave velocity v in the severely aged cable is just 81.5% of that in the unaged cable. Moreover, the trend of wave velocity variation shown in Fig. 8 is in good agreement with the previous theoretical analysis.

The above analysis indicates that for the segmented-aging cable model shown in Fig. 2, when the aging state of segment A is different from that of segment B, the wave velocities in them would be different, which would affect the propagation process of measurement signal and defect location accuracy. In this case, the application of equation (7) in defect location of segmented-aging cables would have its limits, which would lead to the generation of defect location deviation.

D. IMPROVIING DEFECT LOCATION ACCURACY BY CONSIDERING DIFFERENCES IN WAVE VELOCITIES

The above analysis has illustrated that $f'_{x=l} = 2l/v$ is the equivalent frequency of the input impedance spectrum due to the wave reflection at distance l. It should be noted that $2l/v$ is just the time t_l, elapsed for a wave to reach the termination at the distance l and then be reflected back. Similarly, $f'_{x=l1} = 2l_1/v$ is equal to the time t_{l1}, elapsed for a wave to reach the termination at the distance l_1 and then be reflected back. Then the ratio of $f'_{x=l1}$ to $f'_{x=l}$ can be modified and calculated as follows:

$$f'_{x=l_1}/f'_{x=l} == t_{l_1}/t_l \tag{15}$$

where t_{l1} and t_l could be further given by equation (16) and equation (17) for the cable model in Fig. 2.

$$t_{l_1} = 2l_1/v_1 \tag{16}$$

$$t_l = 2\left[l_1/v_1 + (l - l_1)/v_2\right] \tag{17}$$

where v_1 and v_2 are the wave velocities in segment A and segment B, respectively. Combined with equation (15) to equation (17), l_1 could be further calculated again by equation (18).

$$l_1 = \frac{v_1}{v_2 + (v_1 - v_2) \times \frac{f'_{x=l_1}}{f'_{x=l}}} \times l \times \frac{f'_{x=l_1}}{f'_{x=l}} \tag{18}$$

Comparing equation (18) and equation (8), a correction coefficient $M = v_1/[v_2+(v_1\text{-}v_2) \times f'_{x=l1}/f'_{x=l}]$ was defined and put forward, which is considered to be used to reduce the defect location deviation caused by the differences of wave velocities in the segmented-aging cable model in Fig. 2. With introducing M, the defect location deviation of cables with different aging states was calculated again and Table 3 presented the calculation result. By comparing and analyzing the results in Table 2 and Table 3, it is clearly that the defect location deviation is significantly reduced, and the deviation range is narrowed from "−5.13% to 5.13%" to "−0.03% to 0.18%". The result suggests that the defect location accuracy could be improved by considering the difference of wave velocities in segmented-aging cables.

Then the correction coefficient M was further introduced to prove the validity of improve the defect location accuracy in segmented-aging cables with different lengths and with different length percentages of aging segment, respectively, and the modified deviation factors Q were shown in Fig. 9 and Fig. 10. For segmented-aging cables with different lengths,

TABLE 3. Deviation factor Q of cables with different aging states by considering differences in wave velocities.

Deviation factor Q (%)	B1	B2	B3
A1	-	0.11	-0.03
A2	0.18	-	0.01
A3	0.03	0.02	-

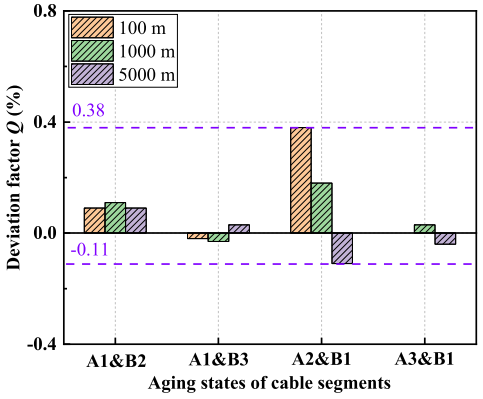

FIGURE 9. Deviation factor Q of cables with different lengths by considering differences in wave velocities.

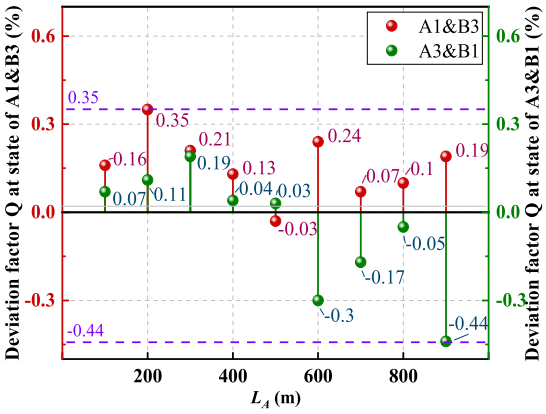

FIGURE 10. Deviation factor Q of cables with different length percentages of aging segment by considering differences in wave velocities.

the deviation range was narrowed from "−5.13% to 5.13%" to "−0.11% to 0.38%". Likewise, for cables with different length percentages of aging segment, the deviation range was also narrowed from "−5.13% to 5.13%" to "−0.44% to 0.35%". These results confirm the defect location accuracy in segmented-aging cables could be improved effectively by considering differences in wave velocities.

IV. EXPERIMENTAL VERIFICATION

A. TEST PLATFORM AND MEASUREMENT PROCESS

A test platform for the segmented-aging cable defect location was built in the laboratory, as shown in Fig. 11. Two cables with different wave velocities were chosen to establish the segmented-aging cable model. The lengths of cable A and

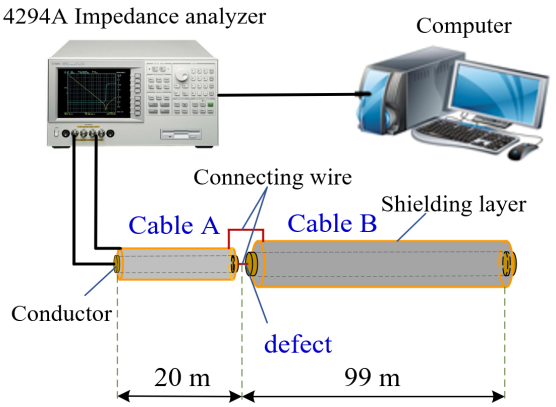

FIGURE 11. Test platform for cable defect location.

cable B were 99 m and 20 m, respectively. Meanwhile, the conductors and the metal shielding layers of cable A and cable B were respectively connected, and the connection point was regarded as the defect.

A 4294A impedance analyzer was used to measure the input impedance amplitude spectrum of the segmented-aging cable model, the ends of two metal conductors (including the conductor and the shielding layer) opposite to the connection point of cable A were connected to two measuring terminals of the analyzer, while that of cable B were kept open. The measuring frequency was in the range of 1MHz to 80 MHz and the sampling points were set to 31600.

In addition, to obtain wave velocities of cable A and cable B, according to the previous measurement procedure, the input impedance amplitude spectra of them were further measured respectively in the range of 1 MHz to 20 MHz, the sampling points were set to 801.

B. COMPARISON OF DEFECT LOCATION ACCURACY BEFORE AND AFTER CONSIDERING THE DIFFERENCE IN WAVE VELOCITIES

The input impedance amplitude spectrum of the segmented-aging cable model was obtained as shown in Fig. 12, and the input impedance amplitude spectra of cable A and cable B were presented in Fig. 13.

Fig. 12 was converted to establish the diagnostic function by FFT, at the same time, the equivalent frequency f' was normalized and the x-coordinate of the peak formed by reflection at the tail end was set to 1, the result was presented in Fig. 14.

It could be obtained easily that the ratio of $f'_{x=l1}$ to $f'_{x=l}$ is 0.19. According to equation (8) and the length of the segmented-aging cable model, the calculated value of l_1 is about 22.61 m. Then it could be deduced the defect location deviation is about 2.19% combined with equation (10).

At the same time, combined with equation (14), the wave velocities of cable A and cable B can be calculated according to Fig. 13, the results are 147 m/μs and 166 m/μs for cable A and cable B, respectively. Based on the results, combined with equation (8) and equation (10), the calculated valve of

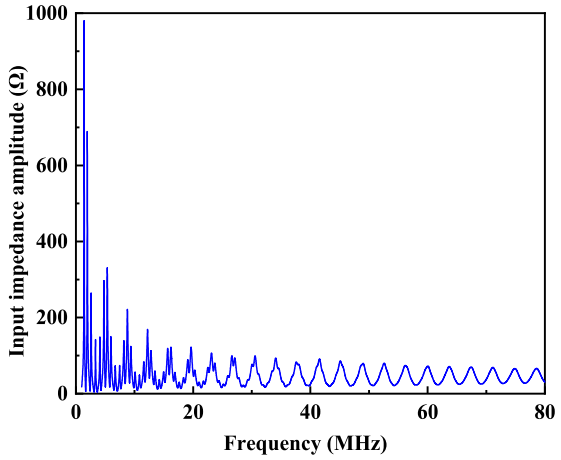

FIGURE 12. Input impedance amplitude spectrum of the segmented-aging cable model.

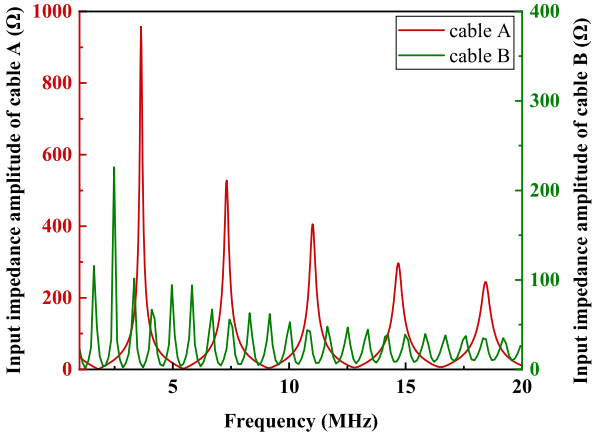

FIGURE 13. Input impedance amplitude spectrum of cable A and cable B.

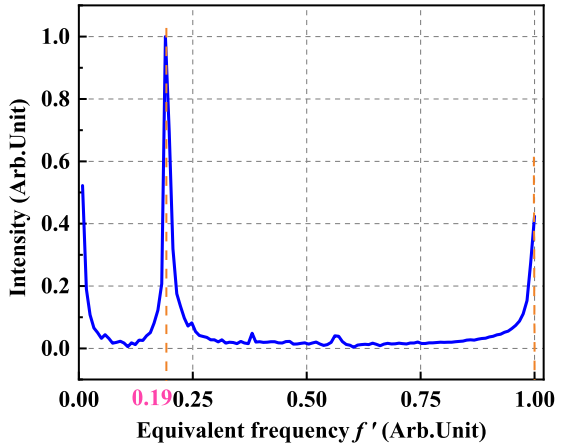

FIGURE 14. Diagnosis function for defect location in the segmented aging cable model.

l_1 is about 20.46 m, and the corresponding defect location deviation is about 0.39%.

The above results show the defect location deviation can be reduced from 2.19% to 0.39% by introducing M. Thus, it can be concluded convincingly that the defect location accuracy

in segmented-aging cables could be improved effectively by considering differences of wave velocities.

V. DISCUSSION

FDR has been proved to be an effective method for defect location in power cables. However, the segmented thermal aging phenomenon in actual XLPE distribution cables is usually not considered in the existing research, which may contribute to the decrease of defect location accuracy.

In this paper, the effect of segmented thermal aging on defect location accuracy in XLPE distribution cables was researched and analyzed through simulation and experiment. The results show that aging states and length percentages of the aging cable segments do have a significant impact on the defect location accuracy, while cable lengths have little influence. The floating range of defect location deviation in the segmented-aging cable models could reach 10% of the whole cable length, thus, it could not be ignored especially for the actual XLPE distribution cables with a length of several kilometers. Further research reveals that the defect location deviation in the segmented-aging cable mainly attributes to the differences of distributed wave velocities caused by the existence of local segmented thermal aging segments. On this basis, a correction coefficient M was introduced to improve the defect location accuracy in the segmented-aging cables model established. Simulation and experimental results show that with the addition of M, the absolute value of defect location deviation is no more than 0.5%. This confirms the validity of improving defect location accuracy in segmented-aging cables by considering the differences of distributed wave velocities.

Meanwhile, it needs to be noticed that how to obtain the distributed wave velocities in XLPE distribution cables is of vital importance for improving defect location accuracy. Since the operation conditions of cables such as the time put into operation, laying environment, replacement messages of local cable segments and so on are almost known, it is possible to classify the cable to several segments according to their aging state roughly, and then the sampling analysis could be carried out to obtain the distribution of wave velocities by measuring the input impedance amplitude spectrum of the sampling segments. In addition, literatures [20] and [22] have proposed a method to locate and determine the degraded segments in a cabled based on the combination of BIS and particle swarm optimization (PSO). This method has achieved some results, however, the defect location deviation caused by the differences of distributed wave velocities was not considered in practice. Thus, the PSO algorithm could be further optimized by taking the differences of distributed wave velocities in cables into accounts, which is of beneficial to improving the defect location accuracy in the end.

VI. CONCLUSION

This paper aims to explore the effect of segmented thermal aging on defect location accuracy in XLPE distribution cables. It can be convincingly concluded that the segmented thermal aging does have an obvious effect on defect location accuracy in XLPE distribution cables, and the floating range of defect location deviation in the segmented-aging cable models could reach 10% of the whole cable length.

Further analysis reveals that the main cause of defect location deviation is the difference of distributed wave velocities, causing by the capacitance change of composite insulation layer of aging cable segments, which is not considered in previous researches. On this basis, a correction coefficient M is proposed to improve the defect location accuracy, and its validity is verified by simulation and experiments, since the absolute value of defect location deviation could be reduced to less than 0.5%. The above results in this paper have some reference value and practical guiding significance for realizing more accurate defect location in actual XLPE distribution cables.

REFERENCES

[1] J. Densley, "Ageing mechanisms and diagnostics for power cables–an overview," *IEEE Elect. Insul. Mag.*, vol. 17, no. 1, pp. 14–22, Jan. 2001.
[2] A. A. Hamad and R. A. Ghunem, "A techno-economic framework for replacing aged XLPE cables in the distribution network," *IEEE Trans. Power Del.*, vol. 35, no. 5, pp. 2387–2393, Oct. 2020.
[3] S. V. Suraci, D. Fabiani, A. Xu, S. Roland, and X. Colin, "Ageing assessment of XLPE LV cables for nuclear applications through physico-chemical and electrical measurements," *IEEE Access*, vol. 8, pp. 27086–27096, 2020.
[4] CIGRE TB 358, "Remaining life management of existing AC underground lines," Paris, France, Tech. Rep. CIGRE WG B1-09, 2007.
[5] Y. Ohki, T. Yamada, and N. Hirai, "Diagnosis of cable aging by broadband impedance spectroscopy," in *Proc. Annu. Rep. Conf. Electr. Insul. Dielectric Phenomena*, Cancún, Mexico, Oct. 2011, pp. 24–27.
[6] T. Yamada, N. Hirai, and Y. Ohki, "Improvement in sensitivity of broadband impedance spectroscopy for locating degradation in cable insulation by ascending the measurement frequency," in *Proc. IEEE Int. Conf. Condition Monitor. Diagnosis*, Bali, Indonesia, Sep. 2012, pp. 677–680.
[7] Q. Shi and O. Kanoun, "Wire fault diagnosis in the frequency domain by impedance spectroscopy," *IEEE Trans. Instrum. Meas.*, vol. 64, no. 8, pp. 2179–2187, Aug. 2015.
[8] Y. Ohki and N. Hirai, "Location attempt of a degraded portion in a long polymer-insulated cable," *IEEE Trans. Dielectr. Electr. Insul.*, vol. 25, no. 6, pp. 2461–2466, Dec. 2018.
[9] M. Xie, K. Zhou, S. Zhao, M. He, and F. Zhang, "A new location method of local defects in power cables based on reflection coefficient spectrum," *Power Syst. Technol.*, vol. 41, no. 9, pp. 3083–3089, Feb. 2017.
[10] X. Rao, K. Zhou, M. Xie, L. Liu, X. Wang, and B. Ye, "Recovery technique of characteristic time domain waveform based on frequency domain reflection method," *High Voltage Eng.*, vol. 47, no. 4, pp. 1420–1427, Apr. 2021.
[11] P. F. Fantoni, "Line resonance analysis system," U.S. Patent 0 228 222 A1, Sep. 10, 2009.
[12] P. F. Fantoni, "Line resonance analysis system," U.S. Patent 7 996 137 B2, Jun. 21, 2011.
[13] Q. Shi, U. Troeltzsch, and O. Kanoun, "Detection and localization of cable faults by time and frequency domain measurements," in *Proc. 7th Int. Multi-Conf. Syst., Signals Devices*, Amman, Jordan, Jun. 2010, pp. 1–6.
[14] N. Hirai, T. Yamada, and Y. Ohki, "Comparison of broadband impedance spectroscopy and time domain reflectometry for locating cable degradation," in *Proc. IEEE Int. Conf. Condition Monitor. Diagnosis*, Bali, Indonesia, Sep. 2012, pp. 229–232.
[15] M. Tozzi, A. Cavallini, G. C. Montanari, and G. L. G. Burbui, "PD detection in extruded power cables: An approximate propagation model," *IEEE Trans. Dielectr. Electr. Insul.*, vol. 15, no. 3, pp. 832–840, Jun. 2008.
[16] Y. Ohki and N. Hirai, "Effects of the structure and insulation material of a cable on the ability of a location method by FDR," *IEEE Trans. Dielectr. Electr. Insul.*, vol. 23, no. 1, pp. 77–84, Feb. 2016.

[17] R. Li, K. Zhou, H. Wan, M. Xie, L. Liu, X. Wang, and M. Miao, "Study on moisture location of cable joints in medium voltage distribution grid based on frequency domain reflection method," *Power Syst. Technol.*, vol. 45, no. 2, pp. 825–832, Dec. 2019.
[18] J. Tian, B. Chen, B. Jiang, R. Li, S. Lei, and H. Hu, "Reconfigurable frequency selective rasorber covering extremely wide transmission frequency range," *IEEE Access*, vol. 8, pp. 225566–225580, 2020.
[19] K. Yu, J. Zeng, X. Zeng, F. Xu, Y. Ye, and Y. Ni, "A novel traveling wave fault location method for transmission network based on directed tree model and linear fitting," *IEEE Access*, vol. 8, pp. 122610–122625, 2020.
[20] Z. Zhou, "Local defects diagnosis for cable based on broadband impedance spectroscopy," Ph.D. dissertation, Dept. Electr. Eng., Huazhong Univ. Sci. Technol., Wuhan, China, 2015.
[21] Y. Ohki, T. Yamada, and N. Hirai, "Precise location of the excessive temperature points in polymer insulated cables," *IEEE Trans. Dielectr. Electr. Insul.*, vol. 20, no. 6, pp. 2099–2106, Dec. 2013.
[22] Z. Zhou, D. Zhang, J. He, and M. Li, "Local degradation diagnosis for cable insulation based on broadband impedance spectroscopy," *IEEE Trans. Dielectr. Electr. Insul.*, vol. 22, no. 4, pp. 2097–2107, Aug. 2015.
[23] A. K. Jonscher, "Dielectric response of polar materials," *IEEE Trans. Electr. Insul.*, vol. 25, no. 4, pp. 622–629, Aug. 1990.
[24] N. Hirai and Y. Ohki, "Highly sensitive detection of distorted points in a cable by frequency domain reflectometry," in *Proc. Int. Symp. Electr. Insulating Mater.*, Niigata, Japan, Jun. 2014, pp. 144–147.
[25] P. Werelius, P. Tharning, R. Eriksson, B. Holmgren, and U. Gafvert, "Dielectric spectroscopy for diagnosis of water tree deterioration in XLPE cables," *IEEE Trans. Dielectr. Electr. Insul.*, vol. 8, no. 1, pp. 27–42, Feb. 2001.
[26] F. Yu and C. Zheng, "Electrodynamics," in *Propagation of Electromagnetic Waves*, 2nd ed. Beijing, China: PKU Press, 2003, pp. 135–170.

BINGLIANG SHAN received the B.S. degree in electrical engineering and automation from North China Electric Power University, Beijing, China, in 2013, where he is currently pursuing the Ph.D. degree. His research interests include aging diagnosis and life evaluation of XLPE distribution cables.

SHUNING LI received the B.S. degree in electrical engineering from North China Electric Power University, in 2019, where she is currently pursuing the M.S. degree. Her research interests include aging diagnosis and defect location in XLPE cables.

LIYING YU (Student Member, IEEE) received the B.E. degree in electrical engineering from North China Electric Power University, in 2020, where she is currently pursuing the M.E. degree. Her research interests include online monitoring and diagnosis of transformer.

WEI WANG received the B.S., M.S., and Ph.D. degrees from North China Electric Power University, in 2001, 2004, and 2012, respectively. He is currently an Associate Professor at North China Electric Power University. His research interests include online monitoring and diagnosis of electrical equipment.

CHENGRONG LI received the B.S. and M.S. degrees in electrical engineering from North China Electric Power University, in 1982 and 1984, respectively, and the Ph.D. degree in electrical engineering from Tsinghua University, in 1989. In 1992, he joined the University of South Carolina, Columbia, SC, USA, as a Postdoctoral Research Fellow. In 1995, he joined North China Electric Power University (NCEPU), where he is currently a Professor with the Department of Electrical Engineering. His research interests include gas discharges, electrical insulation and materials, and condition monitoring of power apparatus.

XIAOKAI MENG received the Ph.D. degree from Dalian University of Technology, in 2017. He is currently working at the Electric Power Research Institute, State Grid Shanxi Electric Power Company. His research interests include high voltage cable insulation state evaluation and fault diagnosis.